Original paper

Magnesiovesuvianite, $Ca_{19}Mg(Al,Mg)_{12}Si_{18}O_{69}(OH)_9$, a new vesuvianite-group mineral

Taras L. PANIKOROVSKII[1]*, Vladimir V. SHILOVSKIKH[2], Evgenia Yu. AVDONTSEVA[1], Andrey A. ZOLOTAREV[1], Vladimir Yu. KARPENKO[3], Anton S. MAZUR[4], Victor N. YAKOVENCHUK[5], Ayya V. BAZAI[5], Sergey V. KRIVOVICHEV[1], Igor V. PEKOV[6]

[1] *Department of Crystallography, St. Petersburg State University, University Emb. 7/9, 199034, St. Petersburg, Russia; taras.panikorovsky@spbu.ru*
[2] *Department of Colloidal Chemistry, Saint-Petersburg State University, University Av. 26, 198504, St. Petersburg, Russia*
[3] *Fersman Mineralogical Museum, Russian Academy of Sciences, Leninskiy Av. 18/2, 115162, Moscow, Russia*
[4] *Center for Magnetic Resonance, St. Petersburg State University, University Av. 26, 198504, St. Petersburg, Russia*
[5] *Nanomaterials Research Centre, Kola Science Centre of the Russian Academy of Sciences, Fersman Str. 14, Apatity, 184200, Murmansk Region, Russia*
[6] *Faculty of Geology, Moscow State University, Vorobievy Gory, 119991 Moscow, Russia*
**Corresponding author*

Magnesiovesuvianite (IMA 2015-104), ideally $Ca_{19}Mg(Al,Mg)_{12}Si_{18}O_{69}(OH)_9$, a new vesuvianite-group member, was found in an old museum specimen labelled as vesuvianite from the Tuydo combe, near Lojane, Republic of Macedonia. It occurs as radiating aggregates up to 2 cm across consisting of acicular tetragonal crystals (up to 7 mm long and 5–40 μm thick) with distinct fibre-optic effect. Associated minerals are calcite, grossular–andradite and clinochlore. Single crystals of magnesiovesuvianite are transparent, light pink with a silky lustre. Dominant crystal forms are {100}, {110}, {101} and {001}. The Mohs' hardness is 6. The measured and calculated densities are 3.30(3) and 3.35 g/cm^3, respectively. Mineral is optically uniaxial, negative, $\omega = 1.725(2)$, $\varepsilon = 1.721(2)$. The chemical composition (wt. % electron-microprobe data) is: SiO_2 36.73, Al_2O_3 20.21, CaO 36.50, MgO 1.80, MnO 0.18, FeO 0.04, Na_2O 0.01, H_2O 3.10, total 98.37. The empirical formula based on 19 (Ca + Na) *apfu* is: $(Ca_{18.99}Na_{0.01})_{\Sigma 19.00}(Mg_{0.60}Al_{0.40})_{\Sigma 1.00}(Al_{11.05}Mg_{0.70}Mn_{0.07}Fe_{0.02})_{\Sigma 11.84}Si_{17.84}O_{68.72}(OH)_9$. Absorption bands in the IR spectrum are: 393, 412, 443, 492, 576, 606, 713, 802, 906, 968, 1024, 3200, 3450, 3630 cm^{-1}. The eight strongest lines of the powder X-ray diffraction pattern are (*I*–*d*(Å)–*hkl*): 23–10.96–110, 22–3.46–240, 33–3.038–510, 100–2.740–432, 21–2.583–522, 94–2.365–620, 19–2.192–710, 25–1.6165–672. Magnesiovesuvianite is tetragonal, space group *P*4/*n*, unit-cell parameters refined from the powder data are *a* 15.5026(3), *c* 11.7858(5), *V* 2832.4(2) Å^3, *Z* = 2. The crystal structure has been refined to $R_1 = 0.027$ for 3266 unique observed reflections with $|F_o| \geq 4\sigma_F$. The structure refinements provided scattering factors of the *Y*1A,B sites close to 12 e^- that supports predominant occupancy of these sites by the Mg^{2+} cations, in perfect agreement with the ^{27}Al MAS NMR data. Magnesiovesuvianite is a member of the vesuvianite group with Mg^{2+} as a dominant cation at the *Y*1 site. The name magnesiovesuvianite is given to highlight the species-defining role of Mg.

Keywords: magnesiovesuvianite, new mineral, light conductor, cation ordering, Lojane, Republic of Macedonia
Received: 16 August, 2016; accepted: 17 February, 2017; handling editor: J. Sejkora
The online version of this article (doi: 10.3190/jgeosci.229) contains supplementary electronic material.

1. Introduction

Due to significant chemical variations and the dependence of the symmetry (space group) upon crystallization temperature (Gnos and Armbruster 2006), minerals of the vesuvianite group seem to indicate conditions of formation and, thus, are of practical interest to geology and geochemistry. Perfect acicular vesuvianite crystals and whiskers show pronounced light-conducting properties (Galuskin et al. 2007). Owing to their structural and chemical complexity, vesuvianite-group minerals are also considered as potential components of silicate materials for the immobilization of dangerous waste products incorporating toxic and radioactive elements such as ^{222}Rn, ^{220}Rn or La (Li et al. 2009; Malczewski and Dziurowicz 2015; Tang et al. 2015).

At present the vesuvianite group consists of six minerals: vesuvianite itself $Ca_{19}(Al,Mg,Mn,Fe)_{13}Si_{18}O_{68}(OH,F,Cl,O)_{10}$ (Werner 1795), wiluite $Ca_{19}(Al,Mg,Fe,Ti)_{13}(B,Al,\square)_5Si_{18}O_{68}(O,OH)_{11}$ (Groat et al. 1998), fluorvesuvianite $Ca_{19}(Al,Mg,Mn,Fe)_{13}Si_{18}O_{68}(F,OH)_{10}$ (Britvin et al. 2003), manganvesuvianite $Ca_{19}Mn^{3+}(Al,Mn^{3+},Fe^{3+})_{10}(Mg,Mn^{2+})_2Si_{18}O_{69}(OH)_9$ (Armbruster et al. 2002), cyprine $Ca_{19}Cu^{2+}(Al,Mg)_{12}Si_{18}O_{69}(OH)_9$ (Panikorovskii et al. in print a) and alumovesuvianite $Ca_{19}Al(Al,Mg)_{12}Si_{18}O_{69}(OH)_9$ (Panikorovskii et al. in print b). Taking into account the modular structure,

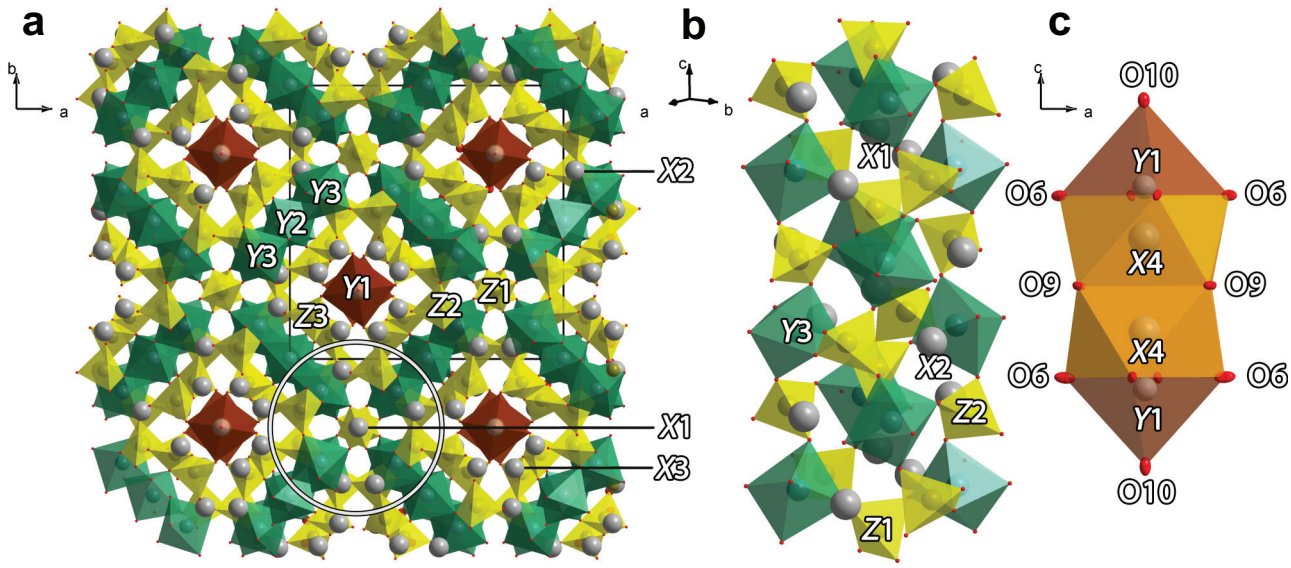

Fig. 1a – A general view of the vesuvianite crystal structure projected along the *c* axis (grossular module highlighted by white circle). **b** – The grossular module in the vesuvianite structure. **c** – Strings of the *Y*1–*X*4–*X*4–*Y*1 positions in the vesuvianite structure.

hydrogarnet-type substitutions, incorporation of sodium and boron, and different cation coordinations, the general formula of vesuvianite-group minerals can be written as $X_{16}X1_2X4Y1Y2_4Y3_8T_{0-5}[(ZO_4)_{10-x}(H_4O_4)_x](Z_2O_7)_4(OH,O)_{10-11}$, where x < 3, *X* are seven- to nine-coordinated sites (Ca, Na, K, Fe^{2+}, *REE*), *X*4 has a square antiprism coordination (Ca, Na), *Y*1 has a square pyramidal coordination (Fe^{3+}, Mg, Al, Fe^{2+}, Cu^{2+}), *Y*2 and *Y*3 have octahedral coordination (Al, Mg, Zn, Fe^{2+}, Fe^{3+}, Mn^{2+}, Mn^{3+}, Ti, Cr, Zn), T_{0-5} (B, Fe or Al) is the additional site with triangular and tetrahedral coordination, whereas ZO_4 (Si, H_4O_4) and Z_2O_7 are ortho- and diortho- groups, respectively (Warren and Modell 1931; Coda et al. 1970; Dyrek et al. 1992; Groat et al. 1992; Armbruster and Gnos 2000b; Galuskin et al. 2003; Aksenov et al. 2016, Panikorovskii et al. 2016a, b, c).

The crystal structure of vesuvianite-group minerals has a modular character (Fig. 1a) and may be considered as containing one-dimensional grossular modules running along the fourfold axis (Allen and Burnham 1992). The modules are linked by the Si_2O_7 groups (Fig. 1b); thereby it forms framework with channels occupied by the *Y*1A,B (*Y*1) and *X*4A,B (*X*4) sites (Fig. 1c) in the *Y*1A–*X*4A–*X*4B–*Y*1B sequence with the distances smaller than 1.3, 1.3 and 2.5 Å between the *Y*1A–*X*4A, *Y*1A–*X*4A and *X*4A–*X*4B positions, respectively. Various occupancies of *Y*1A,B and *X*4A,B positions lead to the different ordering schemes and, as a result, to different space groups (Giuseppetti and Mazzi 1983; Fitzgerald et al. 1986b; Pavese et al. 1998; Armbruster and Gnos 2000a, b).

The majority of vesuvianite samples contain significant amounts of Mg (usually in the range of 0.8–6.7 wt. %), which mostly occupies the octahedrally coordinated *Y*3 positions (Groat et al. 1992). Single crystal X-ray and EXAFS investigations by Valley et al. (1985) and Ohkawa et al. (1992) demonstrated that Mg predominates in the five-coordinated *Y*1 site in vesuvianites from Georgetown, California, USA, and Chichibu, Saitama Prefecture, Japan.

In this paper, we report data for magnesiovesuvianite, ideally $Ca_{19}Mg(Al,Mg)_{12}Si_{18}O_{69}(OH)_9$, a new vesuvianite-group mineral with a predominance of Mg at the *Y*1A,B sites. Both the new mineral and its name have been approved by the IMA Commission on New Minerals, Nomenclature and Classification (IMA 2015-104).

2. Occurrence

Magnesiovesuvianite was found in an old museum specimen from the Tuydo combe, near Lojane, Republic of Macedonia, deposited in the systematic collection of the Fersman Mineralogical Museum of the Russian Academy of Sciences, Moscow, Russia, under catalogue no. 59783 (acquired in 1957). This specimen is considered as the holotype of magnesiovesuvianite.

Associated minerals are calcite, garnet of the grossular–andradite series and clinochlore. The new mineral occurs in cavities of a garnet-bearing rodingite and definitely has a hydrothermal origin.

3. General appearance, physical properties and optical data

Magnesiovesuvianite forms radiating aggregates up to 2 cm across consisting of acicular tetragonal crystals

Fig. 2 Cluster of pink magnesiovesuvianite crystals with fibre-optic effect.

(up to 7 mm long and 5–40 μm thick) with a distinct fibre-optic effect (Fig. 2). This effect is used as a means of transmitting light between the two ends of the fibre, e.g. in computer networking. Crystals are elongated along [001]; the dominant forms are {100} and/or {110}, both usually with striation along [001]; crystals are terminated by the {111} and {101} or {001} faces (Fig. 3). They occur in open cavities or are embedded in fine-grained apple-green garnet.

Magnesiovesuvianite crystals are transparent, light pink, with a silky lustre. Cleavage has not been observed. The Mohs' hardness is 6. The density measured by flotation in diluted Clerici solution (D_{meas}) is 3.30(1) g/cm^3 and calculated using the empirical formula (D_{calc}) is 3.35g/cm^3.

The mineral is optically uniaxial, negative, ω = 1.725(2), ε = 1.731(2) (in white light); pleochroism is not observed. The Gladstone–Dale compatibility index (Mandarino 1981) is –0.018 (superior) for D_{calc} and –0.032 (excellent) if D_{meas} is used.

4. Chemical composition

4.1. Electron microprobe data

Chemical analyses of magnesiovesuvianite (Tab. 1) were obtained by Cameca MS-46 electron microprobe (20 kV, 20–30 nA, beam diameter 10 μm) and by a HITACHI S-3400N scanning electron microscope equipped with the INCA Wave 500 system (WDS mode; 20 kV; 10 nA: beam diameter 5 μm). Contents of other elements with the atomic numbers higher than eight were below the detection limits. The H_2O content was analysed by thermogravimetric analysis (TGA). Carbon dioxide and boron were not analysed because of the absence of bands corresponding to the C–O and B–O vibrations in the IR spectrum. The empirical formula of magnesiovesuvianite, calculated on the basis of 19 (Ca + Na) *apfu* and taking into account the solid-state magic-angle spinning nuclear magnetic resonance (MAS NMR) data, is: $(Ca_{18.99}Na_{0.01})_{\Sigma 19.00}(Mg_{0.60}Al_{0.40})_{\Sigma 1.00}(Al_{11.05}Mg_{0.70}Mn_{0.07}Fe_{0.02})_{\Sigma 11.84}Si_{17.84}O_{68.72}(OH)_9$. The idealized formula is $Ca_{19}Mg(Al,Mg)_{12}Si_{18}O_{69}(OH)_9$, which ideally requires MgO 2.82, CaO 37.13, Al_2O_3 19.54, SiO_2 37.68, H_2O 2.83, total 100.00 wt. %.

Tab. 1 Chemical composition of magnesiovesuvianite (wt. %)

Constituent	Mean	Range	Stand. Dev.	Probe Standard
SiO_2	36.73	36.27–37.35	0.17	SiO_2
Al_2O_3	20.01	19.52–20.67	0.19	Al_2O_3
CaO	36.50	35.80–37.17	0.39	$CaCO_3$
MgO	1.80	1.62–1.99	0.08	MgO
MnO	0.18	0.10–0.36	0.05	Mn
FeO	0.04	0.00–0.23	0.04	Fe
Na_2O	0.01	0.00–0.15	0.04	NaCl
H_2O	3.10			
Total	98.37	96.68–99.33		

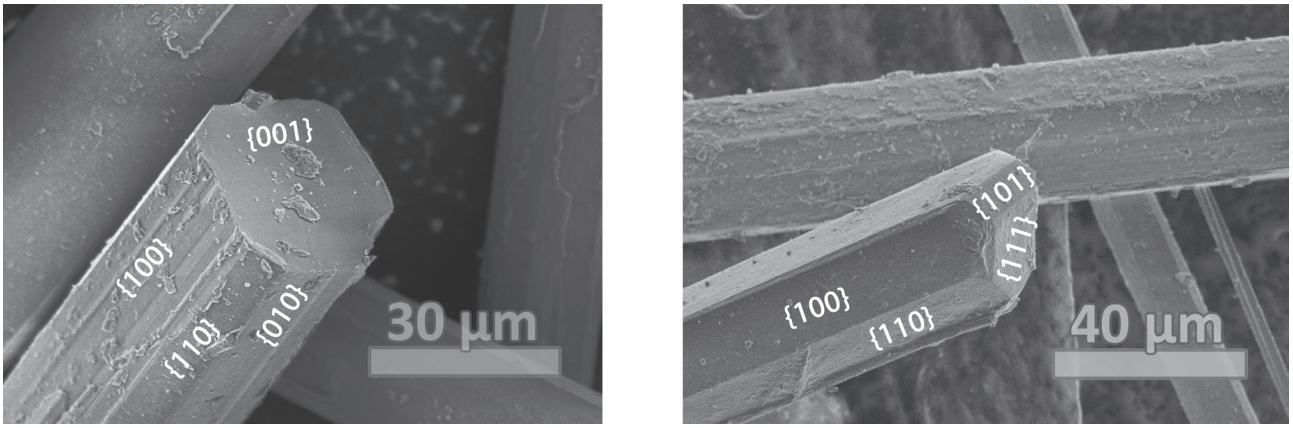

Fig. 3 Back scattered-electron image of two types of acicular crystals of magnesiovesuvianite.

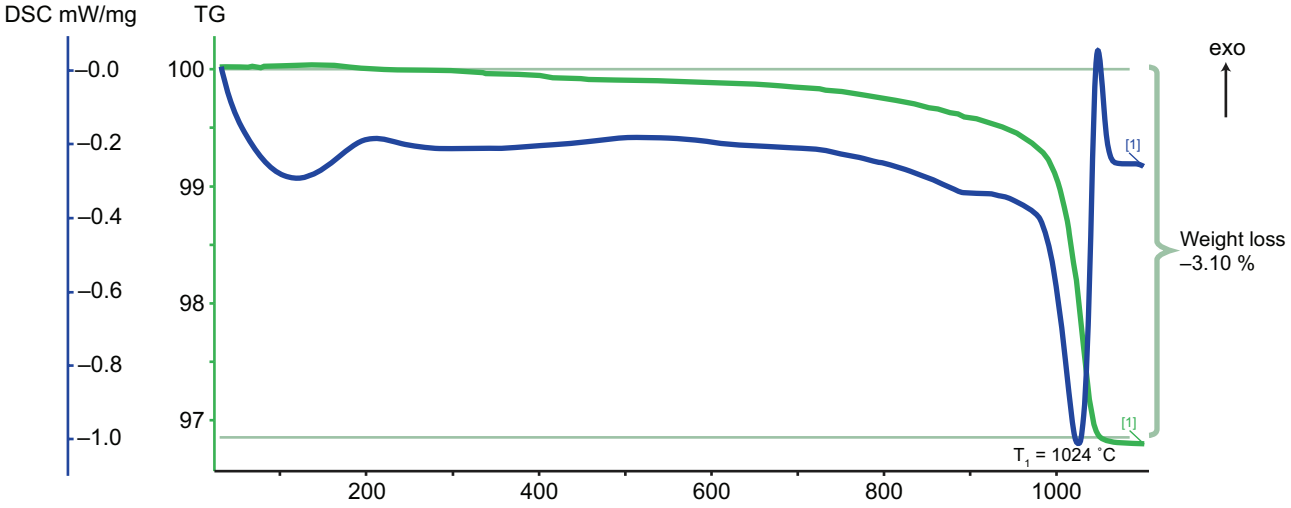

Fig. 4 Thermogravimetric (wt. %, green line) and differential scanning calorimetry (blue line) curves of magnesiovesuvianite.

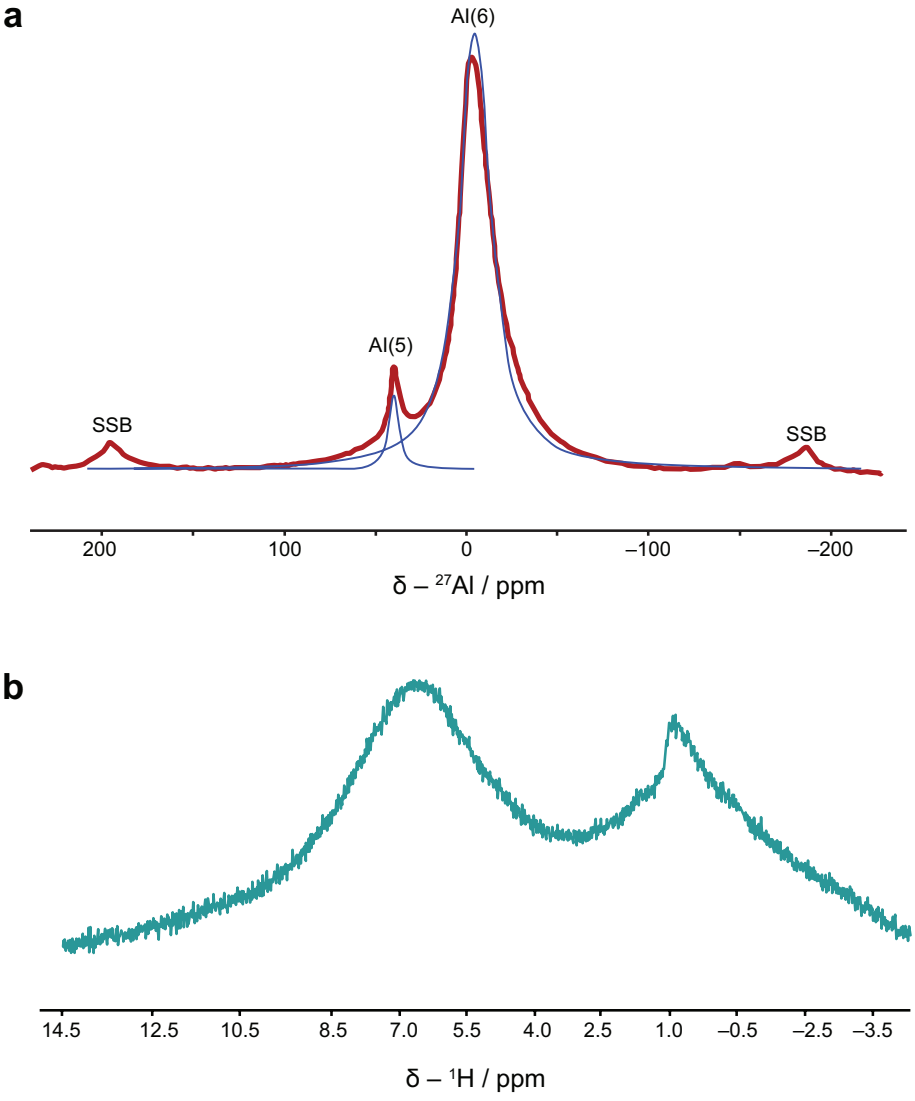

4.2. *Thermogravimetric analyses and differential scanning calorimetry (TGA/DSC)*

This study was performed using a NETZSCH STA 449 F3 Jupiter thermoanalyzer in a dynamic argon atmosphere (heating rate: 10 °C/min, with aluminium oxide standard, sample mass 66.6 mg and temperature range from the room temperature to 1100 °C).

The TGA and DSC curves (Fig. 4) of magnesiovesuvianite have one major step of weight loss, which corresponds to an endothermic effect at 1024 °C and can be assigned to the dehydroxylation process (Földvari 2011). The TGA and DSC curves of magnesiovesuvianite correspond to low-symmetry vesuvianite (*P*4/*n* or *P*4*nc*), which usually has a one-step weight loss with a sharp endothermic peak in the temperature range of 820–1090 °C (Żabiński et al. 1996). Total weight loss for magnesiovesuvianite is

Fig. 5a – ^{27}Al MAS NMR spectrum of magnesiovesuvianite. **b** – ^{1}H MAS NMR spectrum of magnesiovesuvianite.

Tab. 2 Powder X-ray diffraction data for magnesiovesuvianite

I_{meas}	$d_{meas,}$ Å	I_{calc}	$d_{calc,}$ Å	*hkl*	I_{meas}	$d_{meas,}$ Å	I_{calc}	$d_{calc,}$ Å	*hkl*
23	**10.96**	11	10.96	110	2	2.058	2	2.059	254
10	5.48	5	5.48	220	17	2.036	14	2.036	730
2	4.039	9	4.039	231	3	2.020	4	2.020	642
8	3.872	3	3.875	400	5	2.007	5	2.006	731
2	3.653	2	3.654	330	3	1.9930	2	1.9919	363
22	**3.464**	10	3.466	240	6	1.9581	7	1.9573	651
2	3.238	1	3.238	402	3	1.9251	2	1.9275	614
33	**3.038**	12	3.040	510	1	1.9205	9	1.9206	713
9	2.997	8	2.998	431	12	1.8840	10	1.8843	624
9	2.943	6	2.946	004	4	1.7602	2	1.7689	714
100	**2.740**	100	2.753	432	9	1.7120	7	1.7119	910
10	2.658	4	2.658	530	2	1.6751	1	1.6748	734
21	**2.583**	31	2.586	522	4	1.6600	3	1.6593	436
2	2.525	3	2.525	314	25	**1.6165**	18	1.6169	672
3	2.491	3	2.491	611	16	1.5670	12	1.5660	770
94	**2.365**	33	2.366	620	3	1.5551	3	1.5558	616
4	2.320	3	2.319	144	11	1.5184	10	1.5183	655
4	2.265	4	2.267	631	3	1.4930	1	1.4939	844
19	**2.192**	18	2.192	710	2	1.4739	2	1.4729	517
4	2.177	3	2.176	701	3	1.3841	3	1.3828	774
8	2.156	7	2.155	711	5	1.3711	4	1.3719	1004
12	2.117	10	2.116	154	2	1.3500	1	1.3497	1052
2	2.080	1	2.080	623	4	1.3409	3	1.3408	954

3.10 %, which is in good agreement with the calculated H_2O content of 2.83 %.

5. Spectroscopic studies

5.1. Solid-state magic-angle spinning nuclear magnetic resonance (MAS NMR)

5.1.1. ^{27}Al MAS NMR study

The ^{27}Al NMR spectrum was obtained at room temperature by means of a Bruker Advance III 400 WB spectrometer at 104.24 MHz. The MAS spin rate of the rotor was 20 kHz. For these investigations a single-pulse sequence was used with a pulse length of 86 kHz, with recycle delay 1 s and number of scans 4096.

The NMR spectrum (Fig. 5a) of magnesiovesuvianite contains two peaks centred at –3.29 ppm and 39.41 ppm. The peak at –3.29 ppm is in the range of chemical shifts for octahedrally coordinated Al (^{VI}Al). It is assigned to Al at the *Y*2(A,B) and *Y*3(A,B) sites. At the same time the weak peak at 39.41 ppm should be assigned to Al at the 5-coordinated *Y*1(A,B) site. Integral intensities of these peaks are 96.5 to 4.5

Tab. 3 Crystal data, data collection and structure refinement parameters of magnesiovesuvianite

Temperature (K)	293(2)
Crystal system	tetragonal
Space group	*P*4/*n*
a (Å)	15.5362(2)
b (Å)	15.5362(2)
c (Å)	11.7960(3)
α (°)	90
β (°)	90
γ (°)	90
Volume (Å^3)	2847.26(11)
Z	2
D_{calc} (g/cm^3)	3.334
μ (mm^{-1})	2.493
F(000)	2843.0
Crystal size (mm^3)	0.22 × 0.04 × 0.03
Radiation	MoK_α (λ = 0.71073)
2Θ range for data collection (°)	5.066 to 54.996
Index ranges	–7 ≤ h ≤ 20, –19 ≤ k ≤ 11, –15 ≤ l ≤ 7
Reflections collected	6737
Independent reflections	3266 [R_{int} = 0.0143, R_{sigma} = 0.0191]
Data/restraints/parameters	3266/30/305
Goodness-of-fit on F^2	1.240
Final R indexes [I ≥ 2σ (I)]	R_1 = 0.0270, wR_2 = 0.0702
Final R indexes [all data]	R_1 = 0.0292, wR_2 = 0.0712
Largest diff. peak/hole (e Å^{-3})	0.50/–0.48

%. The broad symmetric peaks observed at ± 190 ppm belong to spinning sidebands. It should be noted that very similar data have been reported by Phillips et al. (1987) and Olejniczak and Żabiński (1996), who pointed out that the ^{27}Al MAS NMR spectra for vesuvianites from Asbestos, Canada, and Piz Lunghin, Switzerland, contain two lines corresponding to ^{V}Al and ^{VI}Al.

5.1.2. ^{1}H MAS NMR study

The ^{1}H NMR spectrum was obtained at room temperature using a Bruker Advance III 400 WB spectrometer operating at 400.23 MHz. The MAS spin rate of the rotor was 20 kHz. A single-pulse sequence was used with a pulse length of 100 kHz, recycle delay of 20 s and 32 scans.

The ^{1}H MAS NMR spectrum (Fig. 5b) of magnesiovesuvianite contains two peaks centred at 6.52 and –0.95 ppm in contrast to the spectrum of 'hydrovesuvianite', which contains three peaks centred at 6.74, 3.38 and –0.95 ppm (Panikorovskii et al. 2016c). Absence of the peak at 3.38 ppm indicates the insignificant role of a hydrogarnet $SiO_4^{4-} \leftrightarrow [H_4O_4]^{4-}$ substitution in magnesiovesuvianite. The O–H···O distances calculated using the formula δ_{iso} (ppm) = 79.05 – 0.255d (O–H···O) (pm) (Yesinowski et al. 1988) are 2.84 and 3.13 Å. The most intense peak at 6.74 ppm corresponds to the chemical shifts of the O(11)–H(1*a*)···O(7) and the O(10)–H(2)···O(10) bonds that is in agreement with the distances of 2.784(4) Å and 2.74–2.82 Å, respectively, reported for vesuvianites by many authors (Lager et al. 1999; Ohkawa et al. 1992, 1994, 2009; Pavese et al. 1998; Armbruster and Gnos 2000c; Galuskin 2005). The peak at –0.95 ppm can be attributed to the O(11)–H(1b)···O(11) bond, since its chemical shift agrees with the distances of 3.01–3.04 Å (Pavese et al. 1998; Lager et al. 1999).

5.2. Infrared spectroscopy

The infrared spectrum of magnesiovesuvianite was obtained using a Bruker Vertex 70 IR spectrometer at room temperature (KBr pellet, resolution 4 cm^{-1}). In the IR spectrum (Fig. 6), the absorption bands at 393, 412 and 492 cm^{-1} belong to the $[Al–O]_6$ stretching vibrations. The 443 cm^{-1} band corresponds to the ν_2 symmetric bending vibrations of the Si–O bonds. The bands at 576 and 606 cm^{-1} correspond to the ν_4 asymmetric bending vibrations of the Si–O bonds. A weak band at 713 cm^{-1} may be assigned to vibrations of hydroxyl groups. The bands at 802, 906 (doublet), 968 and 1024 cm^{-1} may be assigned to asymmetric stretching vibrations of Si–O and Si–O–Si bonds. The presence of a doublet with equal intensities of its components (576 and 606 cm^{-1}) corresponding to the ν_4 asymmetric bending vibrations is in agreement with the *P*4/*n* symmetry (Kurazhkovskaya et al. 2003).

The bands in the range 3200–3630 cm^{-1} correspond to O–H stretching vibrations. A band with a maximum at 3630 cm^{-1} in the spectrum of magnesiovesuvianite thus corresponds to the band B (3635)-type. A broad band at 3450 cm^{-1} may belong to the F (3487) and G (3430) bands, which corresponds to the Mg–Al–F and Fe^{2+}–Al–F local configurations of O(11)H site belonging to the trimer of edge-sharing octahedra *Y*2–*Y*3–*Y*2 and this assignment is unlikely due to the absence of F and the low Fe content. The shoulder at 3200 cm^{-1} corresponds to the J (3210) band (O(10)–H stretching vibrations) (Groat et al. 1995) or JK band (Bellatreccia et al. 2005). As shown by Kurazhkovskaya et al. (2003) with Borovikova and Kurazhkovskaya (2006), the presence of the strong band at 3630 cm^{-1} is characteristic of the 'low' vesuvianites, whereas 'high' vesuvianites show a strong band at 3560 cm^{-1}.

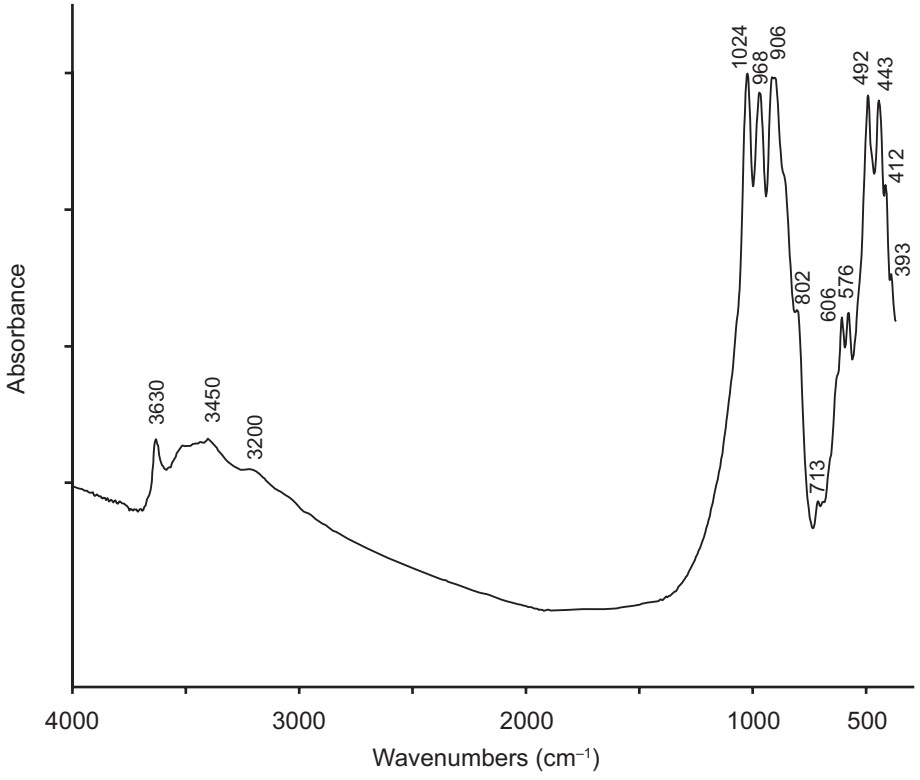

Fig. 6 Infrared spectrum of magnesiovesuvianite.

6. X-ray crystallography

6.1. Powder X-ray diffraction data

Powder X-ray diffraction data (Tab. 2) were collected by a Bruker Phazer D2 diffractometer in the 2θ range of 5–80° (CuK_α; 1.5418 Å) with scanning steps of 0.02° in 2θ. The normal-focus Cu X-ray tube was operated at 40 kV and 30 mA. The unit-cell dimensions determined from the corrected X-ray powder-diffraction by Rietveld refinement using the Topas program (Bruker AXS 2009) are as follows: a = 15.5026(3) Å, c = 11.7856(5) Å, V = 2832.4(2) Å^3.

6.2. Crystal-structure refinement

The single-crystal X-ray diffraction experiment was carried out using an Agilent Technologies Xcalibur Eos diffractometer operated at 50 kV and 40 mA. A hemisphere of three-dimensional data was collected at room temperature using monochromatic MoK_α X-radiation with frame widths of 1° and 80 s count for each frame. For the investigated sample, 208 0kl and hhl reflections were observed that violated the $k + l \neq 2n$ and $l \neq 2n$ absence conditions, indicative of the low symmetry of the crystal structure (Armbruster and Gnos 2000b). Other 14 observed reflections belonged to the hk0 family with $h + k \neq 2n$. The observed systematic absences are consistent with the space group $P4/n$. Attempts to refine the crystal structure in the $P4nc$ space group led to a large number of atoms with physically unrealistic anisotropic displacement parameters.

The crystal structure was refined using a merohedral twin model (2-fold axis along [110]) with the twin ratio 0.485/0.515 to R_1 = 0.027 for 3266 unique observed reflections with $|F_o| \geq 4\sigma_F$ using the *SHELX* program (Sheldrick 2008). Empirical absorption correction was applied in the CrysAlisPro (Agilent Technologies 2014) program using spherical harmonics, implemented in the SCALE3 ABSPACK scaling algorithm. Volumes of coordination polyhedra were calculated using the VESTA 3 program (Momma and Izumi 2011).

Experimental details and crystallographic parameters are given in Tab. 3. The final atomic coordinates and isotropic displacement parameters are in Tab. 4, selected interatomic distances in Tab. 5 and anisotropic displacement parameters in Tab. 6.

Tab. 4 Atom coordinates, displacement parameters (Å^2) and site-scattering factors (*s.s.f.*, $\bar{e}$) for the crystal structure of magnesiovesuvianite

Atom	*apfu*	*x*	*y*	*z*	U_{iso}	*s.s.*	*s.s (calc)*
*Z*1A	$Si_{0.95}[H_4O_4]_{0.05}$	1/4	3/4	0	0.0053(8)	13.34	13.34
*Z*1B	$Si_{0.88}[H_4O_4]_{0.12}$	3/4	1/4	1/2	0.0029(8)	12.32	12.32
*Z*2A	4Si	0.6818(1)	0.4594(1)	0.1297(1)	0.0051(3)	13.55	14
*Z*2B	4Si	0.4583(1)	0.6801(1)	0.3717(1)	0.0045(3)	14.14	14
*Z*3A	4Si	0.34848(9)	0.41410(9)	0.1339(1)	0.0058(3)	13.58	14
*Z*3B	4Si	0.41879(9)	0.34919(9)	0.3642(1)	0.0048(3)	13.94	14
*X*1	2Ca	3/4	1/4	0.2506(1)	0.0053(2)	19.74	20
*X*2A	4Ca	0.54434(7)	0.31139(7)	0.11937(8)	0.0054(2)	19.78	20
*X*2B	4Ca	0.30987(7)	0.54202(7)	0.37878(8)	0.0052(2)	19.76	20
*X*3A	4Ca	0.60084(8)	0.67943(8)	0.11666(8)	0.0126(2)	19.42	20
*X*3B	4Ca	0.68415(7)	0.60320(8)	0.39280(7)	0.0096(2)	19.66	20
*X*4A	$Ca_{0.726(5)}$	1/4	1/4	0.3487(2)	0.0083(7)	14.52	14.52
*X*4B	$Ca_{0.274(5)}$	1/4	1/4	0.1519(6)	0.010(2)	5.48	5.48
*Y*1A	$Mg_{0.194}Al_{0.08}$	1/4	1/4	-0.5434(9)	0.0100(9)	2.87	3.37
*Y*1B	$Mg_{0.406}Al_{0.32}$	1/4	1/4	0.0326(3)	0.0027(5)	8.68	9.03
*Y*2A	2Al	1/2	1/2	0	0.0046(3)	12.87	13
*Y*2B	2Al	1/2	1/2	1/2	0.0048(3)	12.79	13
*Y*3A	$Al_{3.44}Mg_{0.50}Mn_{0.06}$	0.3877(1)	0.6194(1)	0.1261(1)	0.0058(3)	12.60	13.06
*Y*3B	$Al_{3.62}Mg_{0.36}Fe_{0.02}$	0.6219(1)	0.3882(1)	0.3730(1)	0.0054(3)	13.16	12.98
O1A	4O	0.2797(2)	0.6722(2)	0.0864(2)	0.0072(7)		
O1B	4O	0.6713(2)	0.2818(2)	0.4137(2)	0.0068(7)		
O2A	4O	0.6609(2)	0.3825(2)	0.2232(3)	0.0061(7)		
O2B	4O	0.3824(2)	0.6583(2)	0.2793(3)	0.0058(7)		
O3A	4O	0.4504(2)	0.7205(2)	0.0765(3)	0.0065(7)		
O3B	4O	0.7223(2)	0.4505(2)	0.4238(3)	0.0048(7)		
O4A	4O	0.6067(2)	0.4372(2)	0.0306(2)	0.0061(7)		
O4B	4O	0.4371(2)	0.6065(2)	0.4722(2)	0.0064(7)		
O5A	4O	0.3286(2)	0.5123(2)	0.1774(3)	0.0086(7)		
O5B	4O	0.5172(2)	0.3318(2)	0.3199(3)	0.0068(7)		
O6A	4O	0.2708(2)	0.3773(3)	0.0573(2)	0.0141(9)		
O6B	4O	0.3855(2)	0.2702(2)	0.4390(2)	0.0093(7)		
O7A	4O	0.6738(2)	0.5557(2)	0.1812(3)	0.0092(7)		
O7B	4O	0.5557(2)	0.6721(2)	0.3243(3)	0.0080(7)		
O8A	4O	0.4394(2)	0.4075(2)	0.0647(2)	0.0045(7)		
O8B	4O	0.4102(2)	0.4388(2)	0.4328(2)	0.0067(7)		
O9	4O	0.3575(3)	0.3523(3)	0.2496(2)	0.0063(4)		
O10A	$O_{0.54}OH_{0.46}$	3/4	3/4	0.3612(5)	0.011(1)		
O10B	O	3/4	3/4	0.1293(5)	0.012(2)		
O11A	4OH	0.4944(2)	0.5601(2)	0.1375(3)	0.0094(7)		
O11B	4OH	0.5628(2)	0.4960(2)	0.3639(2)	0.0046(7)		

The refined crystal chemical formula is:
$Ca_{19.00}[Al_{11.06}Mg_{0.86}Mn_{0.06}Fe_{0.02}]_{12.00}(Mg_{0.60}Al_{0.40})_{\Sigma 1.00}([SiO_4]_{9.83}[H_4O_4]_{0.17})_{\Sigma 10.00}[Si_2O_7]_4(OH_{8.46}O_{1.54})_{\Sigma 10.00}$

Tab. 5 Selected interatomic distances (Å) for the crystal structure of magnesiovesuvianite

*Z*1A–O1A	1.647(3)	×4	*X*2A–O4A	2.420(3)		<*X*4A–O>	2.483	
			*X*2A–O1A	2.469(4)				
*Z*1B–O1B	1.666(3)	×4	*X*2A–O6A	2.984(4)		*X*4B–O6A	2.293(5)	×4
			<*X*2A–O>	2.468		*X*4B–O9	2.578(4)	×4
*Z*2A–O7A	1.619(4)					<*X*4B–O>	2.436	
*Z*2A–O3A	1.649(4)		*X*2B–O8B	2.326(3)				
*Z*2A–O2A	1.658(4)		*X*2B–O5B	2.341(3)		*Y*2A–O11A	1.874(3)	×2
*Z*2A–O4A	1.688(4)		*X*2B–O3B	2.385(3)		*Y*2A–O8A	1.880(3)	×2
<*Z*2A–O>	1.654		*X*2B–O2B	2.431(4)		*Y*2A–O4A	1.957(4)	×2
			*X*2B–O5A	2.437(3)		<*Y*2A–O>	1.904	
*Z*2B–O7B	1.620(4)		*X*2B–O4B	2.474(4)				
*Z*2B–O3B	1.640(4)		*X*2B–O1B	2.496(4)		*Y*2B–O11B	1.880(3)	×2
*Z*2B–O2B	1.642(4)		*X*2B–O6B	2.822(4)		*Y*2B–O8B	1.865(3)	×2
*Z*2B–O4B	1.678(3)		<*X*2B–O>	2.464		*Y*2B–O4B	1.950(4)	×2
<Z2B–O>	1.645					<*Y*2B–O>	1.898	
			*X*3A–O7A	2.358(3)				
*Z*3A–O6A	1.612(4)		*X*3A–O3A	2.469(4)		*Y*3A–O11A	1.901(4)	
*Z*3A–O8A	1.635(4)		*X*3A–O6A	2.518(3)		*Y*3A–O2B	1.908(3)	
*Z*3A–O5A	1.639(4)		*X*3A–O11A	2.496(3)		*Y*3A–O1A	1.925(4)	
*Z*3A–O9	1.674(4)		*X*3A–O7A	2.505(4)		*Y*3A–O3A	1.939(4)	
<*Z*3A–O>	1.640		*X*3A–O10B	2.568(1)		*Y*3A–O5A	1.994(4)	
			*X*3A–O7B	2.550(3)		*Y*3A–O4A	2.048(3)	
*Z*3B–O6B	1.598(3)		*X*3A–O8A	2.607(3)		<*Y*3A–O>	1.953	
*Z*3B–O8B	1.616(3)		*X*3A–O6A	2.993(3)				
*Z*3B–O5B	1.639(3)		<*X*3A–O>	2.563		*Y*3B–O11B	1.912(4)	
*Z*3B–O9	1.654(4)					*Y*3B–O2A	1.870(3)	
<*Z*3B–O>	1.627		*X*3B–O7B	2.404(4)		*Y*3B–O1B	1.885(4)	
			*X*3B–O3B	2.473(4)		*Y*3B–O3B	1.930(4)	
*X*1–O1A	2.329(3)	×2	*X*3B–O11B	2.538(4)		*Y*3B–O5B	1.951(4)	
*X*1–O1B	2.333(3)	×2	*X*3B–O6B	2.398(3)		*Y*3B–O4B	2.044(3)	
*X*1–O2A	2.502(4)	×2	*X*3B–O7B	2.487(4)		<*Y*3B–O>	1.932	
*X*1–O2B	2.524(4)	×2	*X*3B–O10A	2.527(2)				
<*X*1–O>	2.422		*X*3B–O7A	2.608(3)		*Y*1A–O6B	2.138(4)	×4
			*X*3B–O8B	2.609(3)		*Y*1A–O10A	2.149(13)	
*X*2A–O8A	2.303(3)		*X*3B–O6B	2.996(3)		<*Y*1A–O>	2.140	
*X*2A–O5A	2.334(3)		<*X*3A–O>	2.560				
*X*2A–O3A	2.364(3)					*Y*1B–O6A	2.025(4)	×4
*X*2A–O2A	2.449(4)		*X*4A–O6B	2.380(4)	×4	*Y*1B–O10B	1.910(8)	
*X*2A–O5B	2.423(3)		*X*4A–O9	2.585(3)	×4	<Y1B–O>	2.002	

The tetrahedral *Z*1A,B; *Z*2A,B and *Z*3A,B positions in the crystal structure of magnesiovesuvianite are occupied by Si atoms only. The *Z*1A,B sites demonstrate small Si deficiencies. Both have slightly increased <Z1A–O> and <Z1B–O> distances of 1.647 and 1.666 Å, respectively, and the mean electron counts are 13.3 and 12.3 electrons per formula unit (*epfu*) (for the *Z*1A and *Z*1B positions, respectively) in agreement with the $SiO_4^{4-} \leftrightarrow [H_4O_4]^{4-}$ substitution (Galuskin 2005), which, however, is insufficient to have any influence upon the ^{1}H MAS NMR spectra.

The 7–9 coordinated *X*1, *X*2A,B, *X*3A,B and *X*4A,B sites are fully populated by Ca atoms only. The site occupancies of the eightfold coordinated *X*4A and *X*4B sites in the structure channels (Fig. 1c) are 0.73 and 0.27, respectively.

The principal sites for the identification of magnesiovesuvianite as a new mineral species are the *Y*1A,B sites (Fig. 7) with a square-pyramidal coordination, where Mg prevails over Al. The average <*Y*1A–O> and <*Y*1B–O> bond lengths are 2.140 and 2.002 Å, respectively, which is in agreement with the refined site populations of $Mg_{0.19}Al_{0.08}$ and $Mg_{0.41}Al_{0.32}$, respectively. The site-scattering factor (*s.s.f.*) for the *Y*1 site is 11.55 *epfu* (the calculated value is 12.40 *epfu*), in agreement with the occupancy of the *Y*1A,B sites by Mg only. Considering the MAS-NMR data, the total occupancy of the *Y*1 site requires $(Mg_{0.60}Al_{0.40})_{\Sigma 1.00}$. The *Y*2A and *Y*2B sites are fully occupied by Al, in agreement with the average <*Y*2A–O> and <*Y*2A–O> bond lengths of 1.904 and 1.898 Å, respectively. The average <*Y*3A–O> and <*Y*3A–O> bond lengths

Tab. 6 Anisotropic displacement parameters ($Å^2 \times 10^3$) for magnesiovesuvianite

Atom	U_{11}	U_{22}	U_{33}	U_{23}	U_{13}	U_{12}
*Z*1A	5.6(10)	5.6(10)	4.7(11)	0	0	0
*Z*1B	2.7(10)	2.7(10)	3.5(12)	0	0	0
*Z*2A	7.8(7)	3.4(7)	4.2(6)	–0.2(5)	0.3(5)	–0.8(5)
*Z*2B	6.3(7)	1.1(7)	6.1(6)	0.4(5)	–1.2(5)	0.5(5)
*Z*3A	2.7(7)	8.7(7)	6.0(5)	0.2(5)	–0.3(5)	0.5(5)
*Z*3B	6.5(6)	3.9(7)	4.0(5)	–0.6(5)	–0.1(5)	0.3(5)
*X*1	4.1(3)	5.6(3)	6.5(3)	0	0	–0.3(7)
*X*2A	6.8(5)	4.7(5)	4.8(4)	–0.5(4)	–0.2(3)	1.2(4)
*X*2B	3.4(5)	6.1(5)	6.2(4)	0.4(3)	–1.1(4)	0.2(4)
*X*3A	10.0(6)	9.3(5)	18.4(5)	–4.6(4)	–3.3(4)	4.3(4)
*X*3B	8.3(5)	6.9(5)	13.5(4)	6.8(4)	4.2(4)	1.0(4)
*X*4A	4.2(9)	4.2(9)	16.5(12)	0	0	0
*X*4B	3(2)	3(2)	24(4)	0	0	0
*Y*1A	10.0(8)	10.0(8)	10.2(10)	0	0	0
*Y*1B	2.2(6)	2.2(6)	3.5(7)	0	0	0
*Y*2A	3.7(8)	2.0(8)	8.0(7)	0.3(6)	0.1(7)	0.9(6)
*Y*2B	4.5(5)	4.3(5)	5.5(5)	–0.1(4)	0.3(4)	0.1(4)
*Y*3A	4.8(7)	5.7(8)	6.9(6)	2.4(5)	–2.3(6)	0.4(6)
*Y*3B	5.1(8)	5.6(7)	5.5(6)	–3.8(6)	2.5(5)	–0.8(6)
O1A	12.2(18)	4.0(17)	5.5(13)	2.0(13)	0.2(14)	0.4(14)
O1B	10.2(18)	1.5(16)	8.7(14)	0.6(13)	6.2(14)	–0.4(13)
O2A	5.8(13)	5.8(13)	6.7(12)	0.5(10)	–0.4(10)	–1.7(10)
O2B	5.6(8)	5.6(8)	6.1(7)	0.3(5)	–0.2(5)	0.1(5)
O3A	7.2(17)	5.9(17)	6.5(13)	–1.1(13)	–1.2(13)	1.3(13)
O3B	5.7(17)	4.0(16)	4.7(13)	–1.0(13)	–2.4(12)	–0.7(13)
O4A	1.3(15)	8.5(17)	8.4(15)	3.6(13)	2.0(13)	0.6(14)
O4B	5.5(17)	7.3(16)	6.5(15)	0.3(13)	1.5(13)	0.5(14)
O5A	6.8(17)	12.1(17)	6.9(15)	–0.1(13)	3.5(13)	4.3(14)
O5B	6.1(16)	5.3(16)	8.9(15)	1.2(13)	–1.3(13)	1.1(13)
O6A	5.3(19)	28(2)	8.8(13)	2.2(15)	–0.9(13)	–1.4(15)
O6B	15.0(17)	5.2(18)	7.6(13)	1.6(12)	–0.9(13)	–4.1(13)
O7A	4.5(17)	7.0(17)	16.2(16)	2.3(14)	0.7(14)	0.1(14)
O7B	3.8(16)	15.0(19)	5.1(14)	–2.6(13)	2.1(13)	–0.6(15)
O8A	4.4(8)	4.5(8)	4.6(8)	0.0(5)	–0.2(5)	0.1(5)
O8B	7.5(14)	3.6(13)	8.9(12)	–1.7(10)	0.2(10)	–0.2(10)
O9	6(2)	8(2)	5.0(9)	0.3(12)	0.7(12)	–1.8(8)
O10A	9(2)	9(2)	16(3)	0	0	0
O10B	8(2)	8(2)	22(3)	0	0	0
O11A	9.4(19)	11.3(18)	7.4(13)	0.1(14)	–0.2(14)	–2.0(15)
O11B	5.1(16)	4.3(17)	4.5(13)	0.6(13)	2.7(13)	–0.4(13)

The anisotropic displacement factor exponent takes the form: $-2\pi^2[h^2a \times {}^2U_{11} + 2hka \times b \times U_{12} + \ldots]$

are 1.953 and 1.932 Å, and the calculated occupancy of the *Y*3A and *Y*3B sites are $(Al_{0.86}Mg_{0.125}Mn_{0.015})_{\Sigma 1.00}$ and $(Al_{0.905}Mg_{0.09}Fe_{0.005})_{\Sigma 1.00}$, respectively.

The total crystal-chemical formula for magnesiovesuvianite determined on the basis of crystal-structure refinement and taking account the MAS NMR data can be written as: $(Ca)^{X1}{}_{\Sigma 2.00}(Ca)^{X2A}{}_{\Sigma 4.00}(Ca)^{X2B}{}_{\Sigma 4.00}(Ca)^{X3A}{}_{\Sigma 4.00}(Ca)^{X3B}{}_{\Sigma 4.00}(Ca)^{X4A}{}_{\Sigma 0.73}(Ca)^{X4B}{}_{\Sigma 0.27}(Mg_{0.19}Al_{0.08})^{Y1A}{}_{\Sigma 0.27}(Mg_{0.41}Al_{0.32})^{Y1B}{}_{\Sigma 0.73}(Al)^{Y2A}{}_{\Sigma 2.00}(Al)^{Y2B}{}_{\Sigma 2.00}(Al_{3.62}Mg_{0.36}Fe_{0.02})^{Y3A}{}_{\Sigma 4.00}(Al_{3.44}Mg_{0.50}Mn_{0.06})^{Y3B}{}_{\Sigma 4.00}(Si_{0.95}[H_4O_4]_{0.05})^{Z1A}{}_{\Sigma 1.00}(Si_{0.88}[H_4O_4]_{0.12})^{Z1B}{}_{\Sigma 1.00}(Si)^{Z2A}{}_{\Sigma 4.00}(Si)^{Z2B}{}_{\Sigma 4.00}(Si)^{Z3A}{}_{\Sigma 4.00}(Si)^{Z3B}{}_{\Sigma 4.00}(O)_{\Sigma 68.00}(OH_{8.46}O_{1.54})_{10.00}$.

7. Discussion

There have been several literature reports on Fe-poor vesuvianites, where the content of FeO or Fe_2O_3 did not exceed 1 wt. % (Fitzgerald et al. 1986a, b; Phillips et al. 1987; Groat et al. 1992; Ohkawa et al. 1992; Kurazhkovskaya et al. 2003). According to Hoisch (1985), Groat et al. (1992), Ohkawa et al. (1992), and the present work, vesuvianite incorporates Mg at both octahedral *Y*3A,B and five-coordinated *Y*1A,B positions for structural stability reasons.

It should be noted that, in the crystal structure of vesuvianite, the *Y*1A,B sites are usually occupied by Fe^{3+}

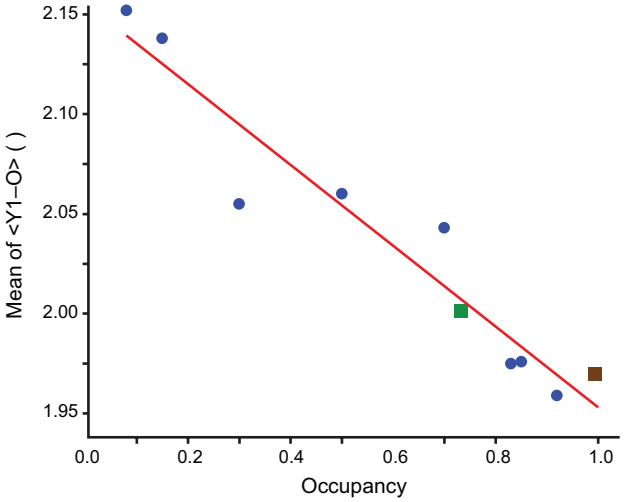

Fig. 7 The mean of <*Y*1–O> vs. occupancy diagram for the Fe^{3+} (blue circles) according to Pavese et al. (1998), Elmi et al. (2011) and Panikorovskii et al. (2016a). Data of present work (green square) and theoretical mean of the 5-coordinated Fe^{3+} according to Shannon (1976) (red square) are also shown.

(Giuseppetti and Mazzi 1983; Panikorovskii et al. 2016a). In Fe-free vesuvianites, the *Y*1A,B sites are occupied by Mg and Al. Their proportion probably depends upon the <*Y*1–O> distance required to stabilize the structure, which is in perfect agreement with compatible <Fe^{3+}–O> distance for the most populated *Y*1A site (Fig. 7).

The most plausible explanation for the occurrence of magnesiovesuvianite (i.e. the incorporation of Mg at the *Y*1 sites) is the absence of significant amount of Fe in the crystallization environment of the mineral. Indeed, the observed striation on the prism faces along [001] is typical of the low-temperature *P*4/*n* vesuvianites of a hydrothermal origin (Armbruster et al. 2002; Gnos and Armbruster 2006). Difference between polyhedral volumes (Tab. 7) of pairs *Y*1A and *Y*1B (7.1179 and 5.8931 Å^3), and *X*4A and *X*4B (24.8468 and 23.8995 Å^3) nonequivalent sites (equivalent in *P*4/*nnc* model) agrees with *P*4/*n* symmetry and low temperature of crystallization magnesiovesuvianite. Therefore, it seems likely that the formation of magnesiovesuvianite was the result of combination of two factors: the relatively high Mg content with the deficit of Fe in the mineral-forming environment from which the mineral crystallized and *P*–*T* conditions of mineral formation.

Tab. 7 Data of polyhedral volumes in the crystal structure of magnesiovesuvianite

Polyhedron	Vol. (Å^3)	Polyhedron	Vol. (Å^3)
*Z*1A	2.2747	*Y*3A	9.8419
*Z*1B	2.3605	*Y*3B	9.5162
*Z*2A	2.2973	*X*1	24.4433
*Z*2B	2.2606	*X*2A	24.5377
*Z*3A	2.2610	*X*2B	24.6638
*Z*3B	2.2035	*X*3A	32.8596
*Y*1A	7.1179	*X*3B	33.0193
*Y*1B	5.8931	*X*4A	24.8468
*Y*2A	9.1105	*X*4B	23.8995
*Y*2B	9.0159		

Acknowledgements. This work was supported by the internal SPbU grant 3.38.136.2014 and the President of Russian Federation Grant for leading scientific schools (no. NSh-10005.2016.5). Experimental studies were carried out using resources of the X-ray Diffraction Centre and Geo Environmental Centre "Geomodel" of Saint-Petersburg State University. Nikita V. Chukanov, Lee A. Groat, an anonymous referee, handling editor Jiří Sejkora and editor-in-chief Vojtěch Janoušek are thanked for critical reviews and helpful comments.The authors are grateful to Gregory Yu. Ivanyuk for the photograph of the magnesiovesuvianite specimen.

Electronic supplementary material. Supplementary crystallographic data for this paper are available online at the Journal web site (*http://dx.doi.org/10.3190/jgeosci.229*).

References

Agilent Technologies (2014) CrysAlis CCD and CrysAlis RED. Oxford Diffraction Ltd, Yarnton, Oxfordshire, UK

Aksenov SM, Chukanov NV, Rusakov VS, Panikorovskii TL, Gainov RR, Vagizov FG, Rastsvetaeva RK, Lyssenko KA, Belakovskiy DI (2016) Towards a revisitation of vesuvianite-group nomenclature: the crystal structure of Ti-rich vesuvianite from Alchuri, Shigar Valley, Pakistan. Acta Cryst B72: 744–752

Allen FM, Burnham CW (1992) A comprehensive structure-model for vesuvianite: symmetry variations and crystal growth. Canad Mineral 30: 1–18

Armbruster T, Gnos E (2000a) *P*4/*n* and *P*4*nc* long-range ordering in low-temperature vesuvianites. Amer Miner 85: 563–569

Armbruster T, Gnos E (2000b) Rod polytypism in vesuvianite: crystal structure of a low-temperature *P*4*nc* vesuvianite with pronounced octahedral cation ordering. Schweiz Mineral Petrogr Mitt 80: 109–116

Armbruster T, Gnos E (2000c) Tetrahedral vacancies and cation ordering in low-temperature Mn-bearing vesuvianites: indication of a hydrogarnet-like substitution. Amer Miner 85: 570–577

Armbruster T, Gnos E, Dixon R, Gutzmer J, Hejny C, Döbelin N, Medenbach O (2002) Manganvesuvianite and tweddillite, two new Mn^{3+}-silicate minerals from the Kalahari manganese fields, South Africa. Mineral Mag 66: 137–150

Bellatreccia F, Della Ventura G, Ottolini L, Libowitzky E, Beran A (2005) The quantitative analysis of OH in

vesuvianite: a polarized FTIR and SIMS study. Phys Chem Miner 32: 65–76

Borovikova EYu, Kurazhkovskaya VS (2006) Influence of fluorine upon formation of ordered and/or disordered modifications of vesuvianite: IR spectroscopy study. Zap Ross Mineral Obsh 135: 89–95 (in Russian)

Britvin SN, Antonov AA, Krivovichev SV, Armbruster T, Burns PC, Chukanov NV (2003) Fluorvesuvianite, $Ca_{19}(Al,Mg,Fe^{2+})_{13}[SiO_4]_{10}[Si_2O_7]_4O(F,OH)_9$, a new mineral species from Pitkäranta, Karelia, Russia: description and crystal structure. Canad Mineral 41: 1371–1380

Bruker AXS GmbH (2009) Topas software, version 4.2

Coda A, Giusta DA, Isetti G, Mazzi F (1970) On the structure of vesuvianite. Atti Accad Sci Torino 105: 1–22

Dyrek K, Platonov AN, Sojka Z, Żabiński W (1992) Optical absorption and EPR study of Cu^{2+} ions in vesuvianite ("cyprine") from Sauland, Telemark, Norway. Eur J Mineral 4: 1285–1289

Elmi C, Brigatti MF, Pasquali L, Montecchi M, Laurora A, Malferrari D, Nannarone S (2011) High-temperature vesuvianite: crystal chemistry and surface considerations. Phys Chem Miner 38: 459–468

Fitzgerald S, Rheingold A, Leavens P (1986a) Crystal structure of a Cu-bearing vesuvianite. Amer Miner 71: 1011–1014

Fitzgerald S, Rheingold A, Leavens P (1986b) Crystal structure of a non-*P*4/*nnc* vesuvianite from Asbestos, Quebec. Amer Miner 71: 1483–1488

Földvari M (2011) Handbook of Thermogravimetric System of Minerals and Its Use in Geological Practice. Occasional Papers of the Geological Institute of Hungary 213: pp 1–180

Galuskin EV (2005) Minerals of Vesuvianite Group from Achtarandite Rocks (Wiluy River, Yakutia). University of Silesia, Katowice, Poland, pp 1–191 (in Polish)

Galuskin EV, Galuskina IO, Sitarz M, Stadnicka K (2003) Si-deficient, OH-substituted, boron-bearing vesuvianite from the Wiluy River, Yakutia, Russia. Canad Mineral 41: 833–842

Galuskin EV, Janeczek J, Kozanecki M, Sitarz M, Jastrzebski W, Wrzalik R, Stadnicka K (2007) Single-crystal Raman investigation of vesuvianite in the OH region. Vib Spetrosc 44: 36–41

Giuseppetti G, Mazzi F (1983) The crystal structure of a vesuvianite with *P*4/*n* symmetry. Tschermaks Mineral Petrogr Mitt 31: 277–288

Gnos E, Armbruster T (2006) Relationship among metamorphic grade, vesuvianite "rod polytypism", and vesuvianite composition. Amer Miner 91: 862–870

Groat LA, Hawthorne FC, Ercit TS (1992) The chemistry of vesuvianite. Canad Mineral 33: 19–48

Groat LA, Hawthorne FC, Rossman GR, Scott TE (1995) The infrared spectroscopy of vesuvianite in the OH region. Canad Mineral 33: 609–626

Groat LA, Hawthorne FC, Ercit TS, Grice JD (1998) Wiluite, $Ca_{19}(Al,Mg,Fe,Ti)_{13}(B,Al,\square)_5Si_{18}O_{68}(O,OH)_{10}$, a new mineral species isostructural with vesuvianite, from the Sakha Republic, Russian Federation. Canad Mineral 36: 1301–1304

Hoisch TD (1985) The solid solution chemistry of vesuvianite. Contrib Mineral Petrol 89: 205–214

Kurazhkovskaya VS, Borovikova EYu, Dorokhova GI, Kononov OV, Stefanovich SYu (2003) IR spectra of high-symmetric and low symmetric vesuvianites. Zap Ross Mineral Obsh 132: 109–121 (in Russian)

Lager GA, Xie Q, Ross FK, Rossman GR, Armbruster T, Rotella FJ, Schultz AJ (1999) Hydrogen-atom position in *P*4/*nnc* vesuvianite. Canad Mineral 37: 763–768

Li H, Ru JY, Yin W, Liu XH, Wang JQ, Zhang WD (2009) Removal of phosphate from polluted water by lanthanum doped vesuvianite. J Hazard Mater 168: 326–330

Malczewski D, Dziurowicz M (2015) ^{222}Rn and ^{220}Rn emanations as a function of the absorbed α-doses from select metamict minerals. Amer Miner 100: 1378–1385

Mandarino JA (1981) The Gladstone–Dale relationship: Part IV. The compatibility concept and its application. Canad Mineral 19: 441–450

Momma K, Izumi F (2011) VESTA 3 for three-dimensional visualization of crystal, volumetric and morphology data. J Appl Crystallogr 44: 1272–1276

Ohkawa M, Yoshiasa A, Takeno S (1992) Crystal chemistry of vesuvianite: site preferences of square-pyramidal coordinated sites. Amer Miner 77: 945–953

Ohkawa M, Yoshiasa A, Takeno S (1994) Structural investigation of high and low-symmetry vesuvianite. Mineral J (Japan) 17: 1–20

Ohkawa M, Armbruster T, Galuskin E (2009) Structural investigation of low symmetry vesuvianite collected from Tojyo, Hiroshima, Japan: implications for hydrogarnet-like substitution. Mineral Petrol 104: 69–76

Olejniczak Z, Żabiński W (1996) ^{27}Al NMR study of white vesuvianite from Piz Lunghin, Switzerland. Mineral Pol 27: 41–45

Panikorovskii TL, Krivovichev SV, Zolotarev AA Jr, Antonov AA (2016a) Crystal chemistry of low-symmetry (*P*4*nc*) vesuvianite from the Kharmankul' Cordon (South Urals, Russia). Zap Ross Mineral Obsh 145: 94–104 (in Russian)

Panikorovskii TL, Krivovichev SV, Yakovenchuk VN, Shilovkikh VV, Mazur AS (2016b) Crystal chemistry of Na-bearing vesuvianite from fenitized gabbroid of the Western Keivy (Kola Peninsula, Russia). Zap Ross Mineral Obsh 145: 83–95 (in Russian)

Panikorovskii TL, Krivovichev SV, Galuskin EV, Shilovskikh VV, Mazur AS, Bazai AV (2016c) Si-deficient, OH-substituted, boron-bearing vesuvianite from Sakha-Yakutia, Russia: a combined single-crystal, ^1H MAS-NMR and IR spectroscopic study. Eur J Mineral 28: 931–941

Panikorovskii TL, Shilovskikh VV, Avdontseva EY, Zolotarev AA, Pekov IV, Britvin SN, Krivovichev SV (in print a) Cyprine, $Ca_{19}Cu^{2+}(Al_{10}Mg_2)Si_{18}O_{68}(OH)_{10}$, a new vesuvianite-group mineral from the Wessels mine, South Africa. Eur J Mineral, doi: 10.1127/ejm/2017/0029-2592

Panikorovskii TL, Chukanov NV, Aksenov SM, Mazur AS, Avdontseva EY, Shilovskikh VV, Krivovichev SV (in print b) Alumovesuvianite, $Ca_{19}Al(Al,Mg)_{12}Si_{18}O_{69}(OH)_9$, a new vesuvianite-group member from the Jeffrey mine, Asbestos, Estrie Region, Québec, Canada. Mineral Petrol, doi:10.1007/s00710-017-0495-1

Pavese A, Prencipe M, Tribandino M, Aagaarel StS (1998) X-ray and neutron single-crystal study of *P4/n* vesuvianite. Canad Mineral 36: 1029–1037

Phillips BL, Allen FM, Kirkpatrick RJ (1987) High-resolution solid-state ^{27}Al NMR spectroscopy of Mg-rich vesuvianite. Amer Miner 72: 1190–1194

Shannon RD (1976) Revised effective ionic radii and systematic studies of interatomic distances in halides and chalcogenides. Acta Crystallogr A32: 751–767

Sheldrick GM (2008) A short history of SHELX. Acta Crystallogr A64: 112–122

Tang XY, Wang SY, Yang Y, Tao R, Dai YV, Dan A, Li L (2015) Removal of six phthalic acid esters (PAEs) from domestic sewage by constructed wetlands. Chem Eng J 275: 198–205

Valley JW, Peacor DR, Bowman JR, Essene EJ, Allard MJ (1985) Crystal chemistry of a Mg-vesuvianite and implications of phase equilibria in the system CaO–MgO–Al_2O_3–SiO_2–H_2O–CO_2. J Metamorph Geol 3: 137–153

Warren BE, Modell DI (1931) The structure of vesuvianite $Ca_{10}Al_4(Mg,Fe)_2Si_9O_{34}(OH)_4$. Z Kristallogr 78: 422–432

Werner AG (1795) Über Vesuvian. Klaproth's Beiträge zur chem Kennt der Mineralkörper, pp 1–34

Yesinowski JP, Eckert H, Rossman GR (1988) Characterization of hydrous species in minerals by high-speed ^1H MAS-NMR. J Am Chem Soc 110: 1367–1375

Żabiński W, Wactawska Z, Paluszkiewicz C (1996) Thermal decomposition of vesuvianite. J Therm Anal 46: 1437–1447